D_{3h} Symmetric Porphyrin-Based Rigid Macrocyclic Ligands for Multicofacial Multinuclear Complexes in a One-Nanometer-Size Cavity

Yohei Ohkoda,[a] Akane Asaishi,[a] Tomoya Namiki,[a] Tomoaki Hashimoto,[a] Midori Yamada,[a] Koichiro Shirai,[a] Yuta Katagami,[a] Tomoaki Sugaya,[a]† Makoto Tadokoro,*[a] and Akiharu Satake*[a]

Abstract: One-step synthesis of D_{3h} symmetric cyclic porphyrin trimers **1** composed of three 2,2′-(4,4′-bismethoxycarbonyl)bipyridyl moieties and three porphyrinatozinc moieties was achieved from a nickel-mediated reductive coupling of *meso*-5,15-bis(6-chloro-4-methoxycarbonylpyrid-2-yl) porphyrinatozinc. Although the cyclic trimers **1** were obtained as a mixture that included other cyclic and acyclic porphyrin oligomers, an extremely specific separation was observed only for cyclic trimers **1** using silica gel columns modified with pyrenylethyl, cyanopropyl and other groups. Structural analysis of the cyclic trimers **1** was carried out using NMR spectroscopy and X-ray crystallography. Treatment of an η^3-allylpalladium complex with a cyclic trimer gave a trispalladium complex containing three η^3-allylpalladium groups inside the space, indicating that the bipyridyl moieties inside the ring could work as bidentate metalloligands.

Introduction

Metal-catalyzed reactions and molecular transformations in nanometer-size cavities[1] are attracting attention in organic synthesis as biomimetic artificial enzymes and metalloenzymes, in which selective reactions are expected to proceed under ambient conditions. On the other hand, bimetallic[2] and multimetallic[2a, 3] catalysts and their related dinuclear[4] and multinuclear[5] metal complexes are also attracting attention because of their high potential for selective transformation and multiredox reactions to activate and transform unreactive and inert molecules and chemical bonds. Therefore, their combined study, i.e., the construction of multimetallic systems with nanometer-size cavities, is a challenging target for the next generation of biomimetic and environmentally benign catalysts in organic synthesis.

Macrocyclic[6] and pseudomacrocyclic[7] multidentate ligands, in which all the coordination sites are directed toward the center of the macrocycle are potential candidates for cofacial dinuclear and multicofacial multinuclear complexes where the metal ions work to manipulate a guest molecule cooperatively. Appropriate spaces to accept desired molecules in macrocycles with their rigid skeletons are required to construct such a reaction field. Macrocyclic porphyrin oligomers are candidates that can serve as multinuclear coordination sites within their rigid skeletons.[8] Macrocyclic porphyrin oligomers are interesting materials for photochemical and electronic organic devices,[9] as well as in the field of molecular recognition[10], selective reactions[1a, 10b] and in ion-transport materials because of their nanometre-size rigid pores.[11] Synthetic strategies for the production of covalently linked cyclic porphyrin oligomers involve either macrocyclization of appropriate length acyclic porphyrin oligomers prepared by multistep synthesis,[10e, 12] or a one-step synthesis from single- or multiple-porphyrin units by coupling reactions in the presence or absence of templates.[13] In both these synthetic approaches, separation of the target cyclic porphyrin oligomer from a mixture that contains other cyclic oligomers and acyclic oligomers is a laborious step that can lead to reduced yield. Gel permeation chromatography (GPC) is a common method that is used to isolate macrocyclic compounds from mixtures. In general, cyclic compounds tend to be eluted later from the GPC column compared with the corresponding acyclic compounds because the hydrodynamic volumes of cyclic compounds are smaller than those of linear compounds.[12b, c, 14] However, the difference is generally small. Therefore, a long column length and/or repeated chromatographic runs are often necessary to isolate the target cyclic oligomer from the mixture.

We have designed new D_3h symmetric macrocyclic ligands **1** for, at most, hexanuclear multicofacial metal complexes, as shown in Figure 1. The ligands of **1** are composed of three 2,2'-bipyridyl moieties and three porphyrinato moieties, and in total, six metal ions can be accepted in the three bidentate ligands and the three tetradentate ligands. To increase the solubility of multinuclear complexes, and also for further functionalization outside the macrocyclic ligands, we planned to introduce six carboxylic ester groups on the 4,4'-positions of each 2,2'-bipyridyl moiety. Because an orthogonal conformation between each porphyrin moiety and the 2,2'-bipyridyl group is predicted, the three porphyrin groups are expected to arrange themselves to produce a three-dimensional prism-shaped space inside. On the *meso*-positions of the three porphyrins, a substituent group (denoted by R in Figure 1) can be introduced during the synthesis of the porphyrin parts. This can be used to control the size of the mouth to the inner space, as well as the size of the inner space. In this study, mesityl and ethyl substituents were examined as a bulky aryl group and a small alkyl group, respectively, denoted by **1a** and **1b** in Figure 1. We planned to achieve the one-step synthesis of **1** by nickel-mediated reductive coupling reaction of bis-2-(6-chloropyridyl) porphyrinatozinc **2** (Scheme 1). The reaction led to the formation of a mixture composed of a target cyclic trimer (C-3mer) and other cyclic and acyclic porphyrin oligomers. During the isolation of C-3mer from

[a] Y. Ohkoda, A. Asaishi, T. Namiki, T. Hashimoto, M. Yamada, K. Shirai, Y. Katagami, T. Sugaya, Prof. M. Tadokoro, and Prof. A. Satake
Graduate School of Chemical Sciences and Technology
Tokyo University of Science
1-3 Kagurazaka, Shinjuku-ku, Tokyo 162-8601, Japan.
E-mail: satake@rs.kagu.tus.ac.jp

Supporting information for this article is given via a link at the end of the document.

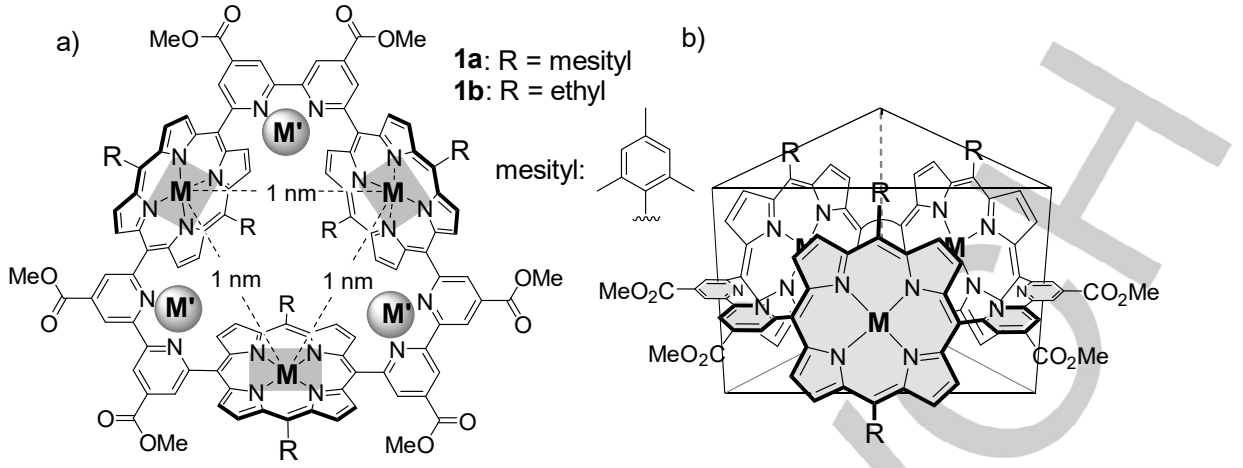

Figure 1. A design of macrocyclic ligand **1** (C-3mer) composed of three 4,4'-methoxycarbonyl-2,2'-bipyridine and three porphyrin groups. ((a) top view, (b) side view) The three 2,2'-bipyridine parts are expected to give metal complexes inside the ring as shown with gray spheres in (a). The six carboxylic acid derivatives outside the ring are expected to increase solubility in various solvent systems. A triangular prism with a triangular space (ca. 1 nm each side) is expected in the orthogonal conformation as shown in (b).

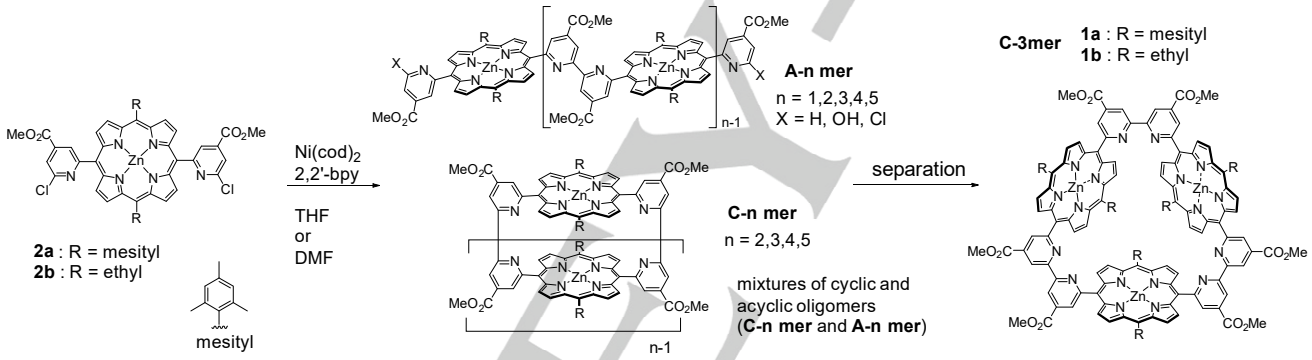

Scheme 1. Synthetic scheme of cyclic trimers (C-3mer) **1a** and **1b**.

the complex mixture, specific retention phenomena were observed by chromatographic analysis with various modified silica-gel columns. Here, we report on this unusual separation behavior, as well as the efficient isolation of the C-3mer **1**, and that the C-3mer has the potential to form versatile macrocyclic ligands for multicofacial multinuclear complexes.

Results and Discussion

Synthesis and isolation of the C-3mer

Porphyrins **2a** and **2b** were synthesized as follows. The corresponding mesityl- or ethyl-substituted dipyrromethanes (**3a** and **3b**) and 6-chloro-4-methoxycarbonylpyridyl-2-paraldehyde **4** were condensed in the presence of trifluoroacetic acid, followed by oxidation with *p*-chloranil to give the freebase porphyrins **5a** and **5b** in 31% and 25% yields, respectively. Incorporation of zinc(II) ions into the freebase porphyrins gave **2a** and **2b** quantitatively (Scheme S1). Referring to our previous conditions for the synthesis of bisporphyrins connected through 2,2'-bipyridyl,[15] nickel-mediated reductive coupling of **2** was performed. Under these conditions, zinc porphyrins and the carboxylic ester moieties in the substrates did not interfere with the reaction. A 1:1 mixture of the bis(1,5-cyclooctadiene)nickel(0) complex ($Ni(cod)_2$, 7–20 equiv.) and 2,2'-bipyridine (7–20 equiv.) was treated with porphyrinatozinc **2** in anhydrous tetrahydrofuran (THF) or anhydrous DMF under an Ar atmosphere at 50 °C for 12 h. When ethyl-substituted **2b** was used as the starting material, the coupling reaction proceeded in THF, and 7 equiv. of the Ni(0)-bpy system was enough to consume most of the starting material. However, in the case of the mesityl-substituted **2a** complex, the conditions discussed above were insufficient, and treatment with 20 equiv. of the Ni(0)-bpy system in the more active solvent DMF[16] gave better results regarding the reproducible consumption of starting materials. After reactions have been completed, the mixture was washed with aqueous ammonium solution to remove the excess

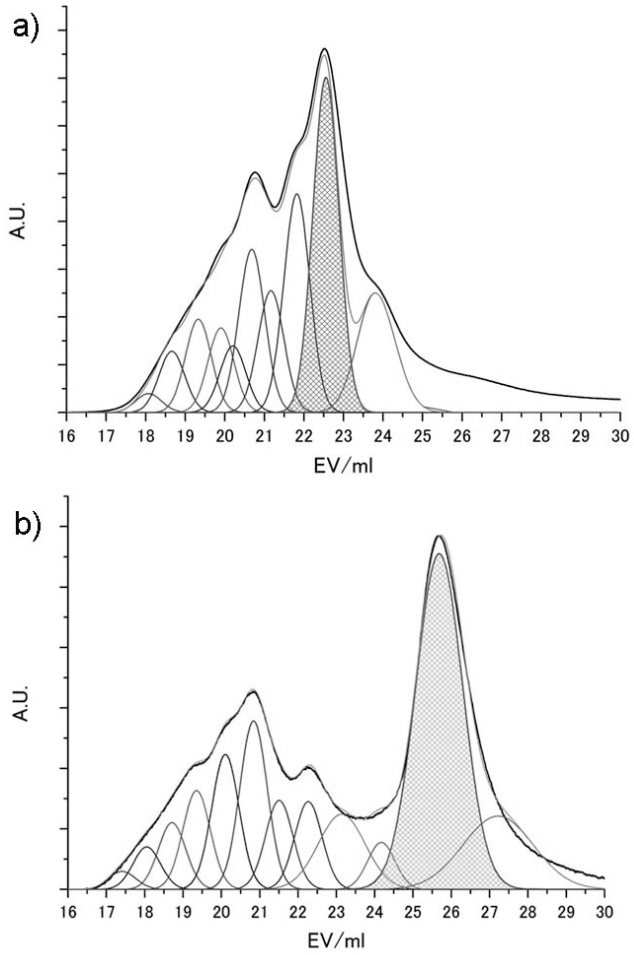

Figure 2. Bold lines in (a) and (b): typical GPC chromatograms of reaction mixtures obtained by nickel-mediated coupling of **1a** (R=mesityl) and **1b** (R=ethyl) (column: TOSOH TSKgel G2500HHR (300 mm (length))×2 (exclusion limit, 20,000 Da) +TOSOH TSKgel G2000HHR (300 mm (length))×1 (exclusion limit, 10,000 Da), eluent: pyridine, flow rate: 1.0~1.2 mL/min), monitored at (a) 556 nm and (b) 566 nm). EV: elution volume, plain lines in (a) and (b): deconvolution analysis of the chromatograms by Gaussian curve fitting using Origin Pro 8 software. The shaded peaks indicate C-3mers, **1a** in (a) and **1b** in (b).

of nickel species, and the organic layer was extracted with $CHCl_3$. The organic layer was analysed with a GPC system fitted with three polystyrene-based GPC columns [two TSKgel G2500 H_{HR} (exclusion limit 20,000 Da, 7.8 mm I.D. × 30 cm) and a TSKgel G2000H_{HR} (exclusion limit 10,000 Da, 7.8 mm I.D. × 30 cm)] connected in series to a photodiode array detector. The elution profiles from the GPC column monitored at 556 and 566 nm, respectively, are depicted as a solid line in Figure 2. Only porphyrin derivatives can be observed at this detection frequency. The plain Gaussian curves shown in Figure 2, which were obtained by deconvolution analysis using Origin 8 software, reveal that more than 10 components containing porphyrin oligomers were present in the crude samples. The ratio of each component varied in each experiment even under the same conditions, and the represented profiles are most typical. In the

Packing Materials	Bonded Phase Structures
C_{18}-MS-II	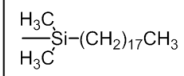
Cholester	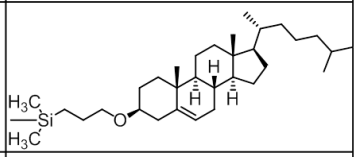
PYE	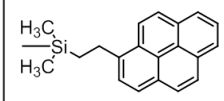
πNAP	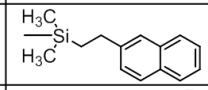
PBB-R	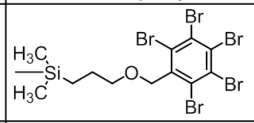
NPE	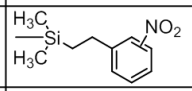
CN-MS	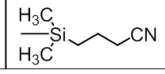

Figure 3. Chemical structures of functional groups bonded on silica gel in modified silica gel columns.

sample analyzed in Figure 2a and 2b, the component eluting at 22.5 mL and 25.6 mL, respectively, (shaded areas, assigned as C-3mer, see below) were obtained as the dominant species. The crude mixture was further separated by using a preparative GPC column packed with polystyrene-based gel [Biorad S-X1 (exclusion limit 14,000 Da), 3 cm diameter × 1 m length], using a mixture of toluene and pyridine (85:15 vol/vol) as eluent under atmospheric pressure. Matrix-assisted laser desorption ionisation time-of-flight mass spectrometry (MALDI-TOF mass) analysis of the fractions showed mass fragments that were approximately two to five times larger than that of the starting monomers **2**, which suggested that the reductive coupling reaction had produced dimeric to pentameric porphyrin oligomers. Some estimated structures are shown in Scheme 1. The terminal moieties of acyclic porphyrin oligomers, indicated as X in A-n mer in Scheme 1, were assigned as H, Cl or OH, but some unidentified signals were also observed in the MALDI-TOF mass analyses.

The following detailed analysis describes the case of using ethyl-substituted **2b** as a starting material for the coupling reaction. In the GPC chromatographic separation, compounds corresponding to the trimer were detected in two fractions, with the later eluting compound assigned as the target C-3mer **1b** based on high-resolution MALDI-TOF MS analysis. However, in addition to the target C-3mer **1b**, the fraction contained other monomeric and dimeric porphyrin derivatives, thus further

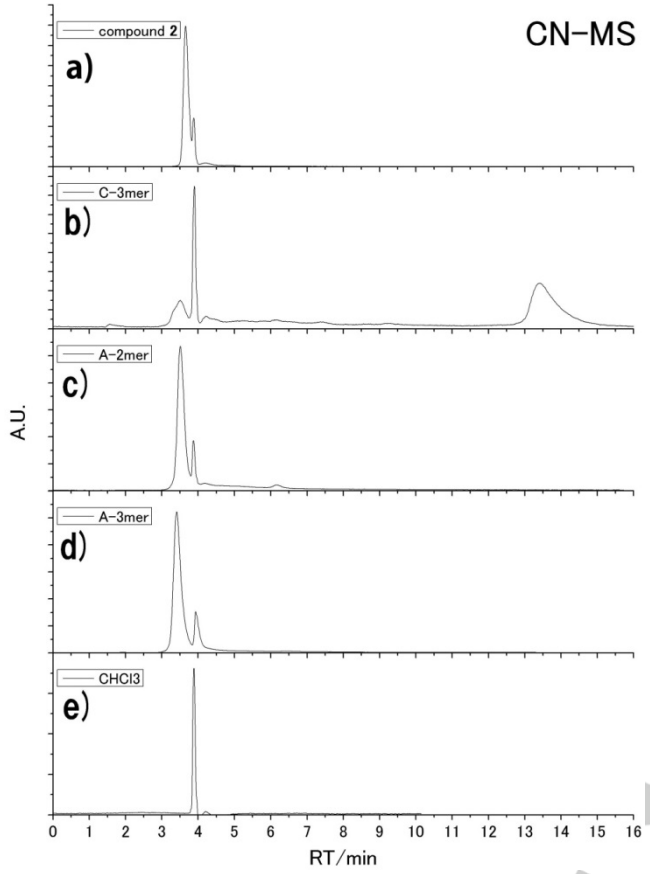

Figure 4. Chromatograms of (a) compound **2b**, (b) C-3mer, (c) A-2mer, (d) A-3mer and (e) chloroform with analytical HPLC column CN-MS (4.6 mm (ID), 15 cm (length)). A mixture of toluene and pyridine (15:85 vol/vol) was used as an eluent.

purification was required. Although a recycling GPC method could be used to isolate the C-3mer **1b**, other chromatographic techniques involving modified silica gel were surveyed to find a more efficient method. Four analytes, compound **2b** and three fractions containing mainly acyclic dimer (ethyl A-2mer), acyclic trimer (ethyl A-3mer) and cyclic trimer (ethyl C-3mer) were prepared to compare the elution behaviour in various modified silica-based columns. Eight HPLC columns (COSMOSIL® series), C18-MS-II, Cholester, PYE, πNAP, NPE, PBB-R, NPE and CN-MS (4.6 mm I.D. × 15 cm) supplied by Nacalai Tesque were tested. The chemical structures of the functional groups on these columns are shown in Figure 3. Thus, octadecyl, cholesterol ether, pyrenylethyl, naphthylethyl, pentabromobenzyl ether, nitrophenylethyl and cyanopropyl moieties were attached to silica gel (5 μm particle, 120 Å pore). GPC and MALDI-TOF MS analyses of the four analytes used here are shown in Figures S1–S4. A mixture of toluene and pyridine was used as eluent. The polarity parameters of the solvents were 2.3 (toluene) and 5.3 (pyridine);[17] therefore, the combination of these solvents worked well to elute all of the analytes without adsorption in the stationary phase.

Table 1. Retention factors (*k*) of compounds on modified silica-gel HPLC columns.

Run	Column	retention factors[a]		
		k_{2b}	k_{CHCl3}	$k_{\mathrm{C3mer\ 1b}}$
1	CN-MS	0.08	0.14	2.95
2	C_{18}-MS-II	0.08	0.25	0.04
3	Cholester	0.08	0.24	0.02
4	πNAP	0.08	0.12	0.88
5	PBB-R	0.08	0.10	0.94
6	PYE	0.10	0.10	1.68
7	NPE	0.09	0.14	3.03

[a] $k = (t\text{-}t_0)/t_0$; t_0: retention time of A-3mer

Chromatograms of the analytes obtained by column chromatography with CN-MS as stationary phase are shown in Figure 4a–d; as a reference, a chromatogram of 10 μL of chloroform is also illustrated in Figure 4e. The peak at 3.88 min in each chromatogram in Figure 4a–d is a shock peak of chloroform used for dilution of the analytes. Peaks of compound **2b**, A-2mer and A-3mer eluted earlier than the shock peak, which suggested that almost no retention occurred under these conditions, with the A-3mer eluting earliest. In contrast, C-3mer eluted much later (13.4 min) than those peaks, and impurities contained in this analyte eluted earlier (3~11 min) than C-3mer. These results indicated the specific interaction of C-3mer with silica gel modified by cyanopropyl groups.

If we assume that A-3mer was not retained on the CN-MS column at all, then the retention time of this compound can be defined as t0. Retention factors, $k = (t - t_0)/t_0$, can be calculated based on t_0 as shown at Run 1 in Table 1. Here, k_{2b}, k_{CHCl3} and $k_{C\text{-}3mer\ 1b}$ are the retention factors of compounds **2b**, $CHCl_3$ and C-3mer **1b**, respectively. If a retention factor (*k*) is larger than 1, the retention time of the analyte is more than two times longer than that of A-3mer. The large difference in the retention times of A-3mer and C-3mer is noteworthy. Other chromatograms using C18-MS-II, Cholester, PYE, πNAP, PBB-R and NPE are shown in Figures S5–S7. In the case of C18-MS-II and Cholester, C-3mer **1b** was not retained as well as **2b**, A-2mer and A-3mer (Figure S5). In contrast, specific retention of C-3mer **1b** was observed in PYE, πNAP, NPE and PBB-R columns (Figures S6 and S7). In all of the chromatograms, A-3mer eluted first, and the retention times of A-3mer can be defined as t_0. Retention factors *k* are listed in Table 1. The retention factors of C-3mer in C18-MS-II and Cholester were 0.04 and 0.02, respectively, which are similar to those of porphyrinatozinc **2b** and C-3mer **1b**, suggesting that no interaction was observed between C-3mer **1b** and the stationary phase in C18-MS-II and Cholester. The retention factors of C-3mer **1b** in PYE, πNAP and PBB-R were in the range 0.88–1.68, whereas that of **2b** remained below 0.1, which indicated that a specific interaction between C-3mer **1b** and the stationary phase was observed.

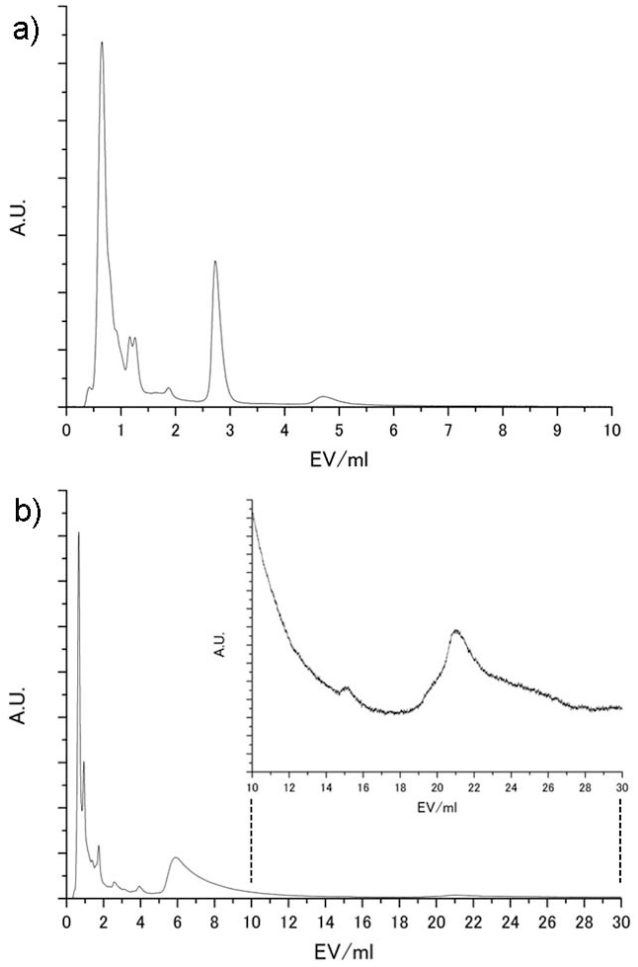

Figure 5. (a) and (b): chromatograms of reaction mixtures obtained by nickel-mediated coupling of **1a** (R=mesityl) and **1b** (R=ethyl) by using a Nacalai tesque 5CN-MS HPLC column ((4.6 mm (ID) × 50 mm (length)), eluent: toluene / pyridine = 15 / 85 (vol/vol), flow rate: 0.5 mL/min, monitored at 556 nm. Peaks at 2.7 mL in (a), and 6 mL in (b) correspond to **1a** and **1b**, respectively. Inset in (b): magnified chart from 10 to 30 mL for elution volume. The same samples were used in Figures 2(a) and 5(a), and Figures 2(b) and 5(b), respectively.

Larger retention factors for C-3mer (ca. 3) were observed with NPE and CN-MS, and the retention factors of k_{2b} remained below 0.1. For comparison, thin-layer chromatographic (TLC) analysis was performed with an unmodified SiO_2 plate with a mixture of toluene/pyridine (15:85) as eluent; in this case, all of the analytes (**2b**, A-2mer, A-3mer and C-3mer) eluted to the top of the plate (R_f=1), indicating that almost no interaction of the analytes with the silanol residues occurred with this solvent system. The specific separation mechanism of C-3mer **1b** on some modified silica gel columns is discussed in later parts. After the survey, cyanopropyl-modified silica gel chromatography was selected for use in the more efficient separation of cyclic trimers from the crude reaction mixtures. In Figures 5a and 5b, chromatogram charts of the reaction mixtures of the C-3mers synthesized from **2a** and **2b** using a shorter CN-MS column (ID = 4.6 mm × 50 mm) are shown. The reaction mixtures are the same samples that were analyzed using the GPC systems shown in Figures 2a and 2b. The peaks occurring at 2.8 mL and 6 mL in Figures 5a and 5b, respectively, correspond to the cyclic trimers **1a** and **1b**. These were eluted much later than most of the other oligomers, even from the crude reaction mixtures. The tailing behavior observed in the ethyl-substituted cyclic trimer **1b** suggests a stronger interaction with cyanopropyl moieties than that with the mesityl-substituted cyclic trimer **1a**. The peaks that eluted later than the cyclic trimers, at 4.7 mL (Figure 5a) and at 21 mL (Figure 5b), were assigned to a mesityl-substituted monohydrolyzed cyclic trimer (Figures S8 and S9) and an ethyl-substituted cyclic tetramer (Figure S10), respectively, from their MALDI-TOF mass analysis. Finally, preparative chromatographic separation of both mesityl- and ethyl-substituted cyclic trimers, **1a** and **1b** from the corresponding crude reaction mixtures, was carried out on silica gel modified with cyanopropyl groups (Cyanogel) purchased from the Yamazen Corporation for flash chromatography. These were purified using Cyanogel chromatography employing a mixture of pyridine and toluene (85:15) as eluent. This purification method was much easier than that using the GPC method. Any used cyanopropyl-modified silica gel was reused several times to purify different crude mixtures. After purification using Cyanogel column chromatography, the ethyl-substituted C-3mer **1b** was washed with a 0.3 M aqueous citric acid solution and then with deionized water in $CHCl_3$. The concentrated organic layer was further purified using unmodified SiO_2 column chromatography employing $CHCl_3$ and ethyl acetate (5:1) as eluents to give 1b in a 9.0% isolated yield. The mesityl-substituted C-3mer **1a** was further purified by recrystallization from 2-butanone and methanol, after Cyanogel column purification, to give **1a** in a 13.1% isolated yield.

NMR structural analysis of the C-3mers

NMR structural analysis of cyclic trimers **1a** and **1b** was carried out. The ^{1}H NMR spectrum of **1a** and that of the corresponding monomeric zinc porphyrin **2a** in $CDCl_3$ are shown in Figures 6a and 6b. Similar to the spectrum of **2a**, the spectrum of the C-3mer **1a** showed only a single set of signals, which indicated that **1a** has a D_3h symmetric structure. All the signals of **1a** could be assigned, as shown in Figure 7, using 2D NMR techniques: heteronuclear multiple quantum coherence (HMQC), and heteronuclear multiple bond connectivity (HMBC) (Figures S11–S14). Similar to the ^{1}H NMR spectrum of **1a**, the spectrum of **1b** also showed simple signals, indicating that **1b** had a D_3h symmetric structure (Figure S16). In the case of the ^{1}H NMR spectrum of **1b**, coordinated pyridine molecules were observed at 4.3, 3.8, and 2.2 ppm as broad signals. The source of the pyridine molecules was the eluent that was used in the Cyanogel column chromatography. Because the ^{1}H NMR spectrum of **1b** changed slightly depending on the amount of pyridine molecules in the $CDCl_3$, an NMR structural analysis of **1b** was performed in pyridine-d_5. All the 1D and 2D NMR data and assignments of **1b** in pyridine-d_5 are shown in Figures S18–S23. In the case of **1a**, no residual pyridine was observed in the NMR spectra.

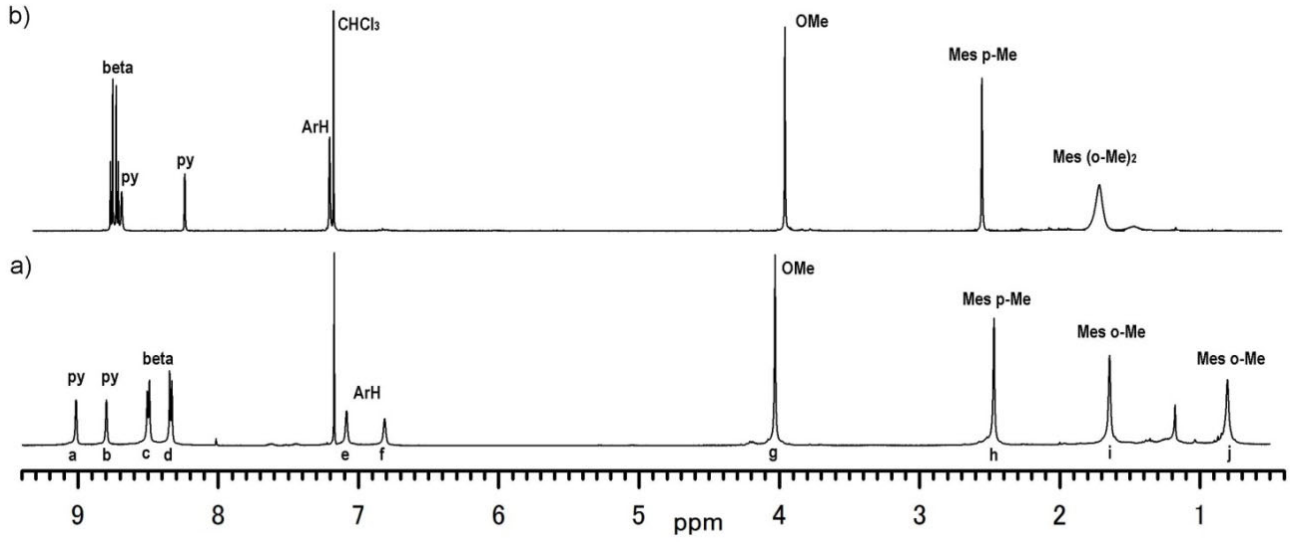

Figure 6. ^{1}H NMR spectra (300 MHz, in $CDCl_3$) of (a) **1a** and (b) **2a**. Assignment of the signals [a – j] from lower to upper fields in the NMR spectrum (a) correspond to [a – j] in Figure 7.

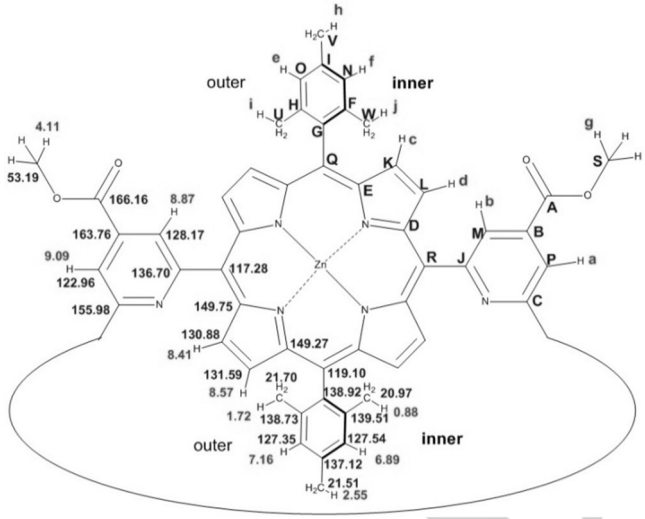

Figure 7. Assignments of ^{1}H (300 MHz) and ^{13}C NMR (75 MHz) signals of cyclic trimer **1a** in $CDCl_3$..

*X-ray crystallography of the C-3mer **1a***

The molecular structure and the ORTEP model of the C-3mer **1a** are shown in Figures 8 and S24, respectively. A deformed triangular prism shape was observed, in which all six methyl ester groups were directed toward the outside, whereas the nitrogen atoms on the bipyridyl groups were directed toward the inside. The distance between the two zinc ions was 9.64–9.70 Å (Table 2), indicating that C-3mer **1a** has a one-nanometer-size space inside. Although the D_{3h} symmetry of **1a** was observed in the ^{1}H NMR data, a C_s symmetric structure was observed in the crystal structure because of the incline in one of the three porphyrin groups in **1a,** which allows it to interact with a bipyridyl moiety in a neighboring cyclic porphyrin **1a**. The bipyridyl (C(17)–C(21)) and mesityl (C(67)–C(69)) moieties on the symmetric plane passing through the Zn(2), C(66), C(70), and C(71) atoms are disordered, as shown in Figure S24. The angle of the porphyrin plane tilted away from the perpendicular of the mean plane containing the three 2,2'-bipyridyl parts is 31°(Figure 9). This result suggests that, in solution, the porphyrin moiety in **1a** can rotate approximately ±30°along the axis through the two *meso*-positions connected to the two pyridyl parts.

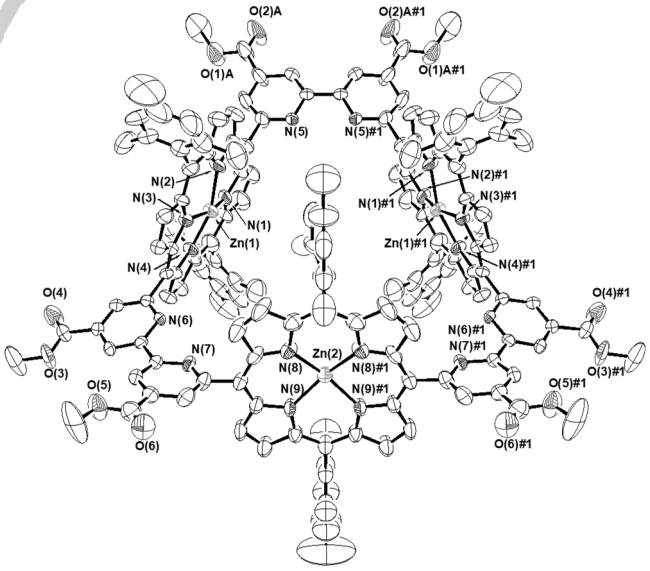

Figure 8. The ORTEP drawing of **1a**. Ellipsoids are drawn at their 50% probability level; hydrogen atoms, coordinated methanol molecules, and

disordered moieties were omitted for clarity. Symmetry transformations used to generate equivalent atoms: #1 x, -y+1/2, z

Table 2. Zn center distances (Å) for **1a**. [a]

bond	distance
Zn(1)-Zn(2)	9.6404(12)
Zn(1)-Zn(1)#1	9.7046(16)

[a] Symmetry transformations used to generate equivalent atoms: #1 x, -y+1/2, z

Mechanisms of specific separations of C-3mer on modified silica gel columns

From the chemical structures of the modified columns shown in Figure 3 and the retention factors of C-3mer **1b** on the columns listed in Table 1, the columns can be classified into three groups. Two columns, C18-MS-II and Cholester, have nonaromatic acyclic and cyclic residues, and they have almost no retention capability for C-3mer **1b** (< 0.04). These columns are classified as group A. Three columns: PYE, πNAP, and PBB-R, have nonpolar aromatic residues, and their retention capability for C-3mer **1b** is moderate (0.88–1.68). These columns are classified as group B. The last two columns: NPE and CN-MS, have polar residues, and they retained C-3mer **1b** the most strongly (ca. 3.0). These columns are classified as group C. Because of the difference in the chemical structure between groups B and C, the mechanism of their specific separation was considered to be different.

To discuss these mechanisms, the effect of the solvent eluent was examined. When chloroform was used as an eluent on the NPE column (group C), acyclic ethyl A-3mer and C-3mer **1b** were adsorbed on the column and were not eluted within retention time (RT) 30 min, whereas monomeric **2b** was eluted at RT 4 min immediately (Figure S25). Increasing the polarity of the eluent using a toluene/pyridine system on the NPE column caused an immediate elution of ethyl A-2mer and ethyl A-3mer, followed by a significantly delayed elution of C-3mer **1b** (Figure S26). These observations are explained by the dipole–dipole interactions between nitrobenzene moieties on the NPE column and the functional groups on the ethyl A-2mer, ethyl A-3mer, and C-3mer **1b**. Because of the restricted conformation of the 2,2'-bipyridyl groups of the C-3mer, the partial dipole moment must be larger than the 2,2'-bipyridyl groups on the ethyl A-2mer and ethyl A-3mer, which can assume a different conformation by rotating along the C–C bond between the two adjacent pyridyl moieties. Pyridine is considered to be a polar solvent that cancels out the relatively weak dipole–dipole interactions between the nitrobenzene moieties and the ethyl A-2mer and ethyl A-3mer, and only the strong dipole–dipole interactions with the NPE column for C-3mer **1b** were observed even in polar pyridine. However, on a pyrene-modified column (PYE), chloroform acted in an entirely different manner. Thus, when chloroform was used as an eluent on a PYE column (group B), both the ethyl A-3mer and the C-3mer **1b** were eluted immediately with slight tailing. The retention times of the peak maxima were earlier than that of **2b** (Figure S27). The specific retention of C-3mer **1b** on a PYE column was only observed when pyridine was used as an eluent, as shown in Figure S6a. This observation suggests that chloroform suppresses any interaction between the pyrenyl groups on the PYE column and C-3mer **1b**, whereas pyridine helps the interaction of the PYE column and C-3mer **1b**. To obtain information on the interaction of chloroform with C-3mer **1b**, pyridine-free C-3mer **1b** was prepared by washing it with citric acid solution several times until any residual pyridine was removed completely.

The ^{1}H NMR spectrum of pyridine-free C-3mer **1b** in $CDCl_3$ exhibited very broad signals, which indicated that conformational isomers existed and that the exchange rate among the isomers was slow on the NMR timescale (Figure S28). The broad signals became sharp with D_3h symmetry in the presence of trace amounts of pyridine or when only pyridine-d_5 was used (Figures S16 and S18).

These NMR observations can be explained by the chloro-form molecules being held tightly within the C-3mer with several conformational arrangements and the exchange rate among the conformers being slow. A coordinating solvent, such as pyridine, probably increases the rate of conformational exchange by a rapid coordination exchange between the ligand and the zinc ion, and during this process, the chloroform molecules held within the C-3mer are ejected from the inside.

To represent the chromatographic conditions of a PYE column with pyridine, a ^{1}H NMR titration experiment of C-3mer **1b** in the presence of *N*-methylimidazole (**Im**) with pyrene was carried out (Figure S29). *N*-methylimidazole was used instead of pyridine because the association constant of zinc tetraphenylporphyrin is larger (logK = 4.66) than that of pyridine (logK = 3.52)[18], and monitoring the ^{1}H NMR signal of *N*-methyl part was applicable. A mixture of C-3mer **1b** (3.6 mM) and ca. 20 equiv of **Im** in $(CDCl_2)_2$ was prepared. Under these conditions, all the zinc moieties had to have been coordinated with **Im** from both the inside and outside of the C-3mer to give five-coordinated **Im**-zinc porphyrin complexes (B in Figure S29). The ^{1}H NMR spectrum obtained is shown in Figure S30, and a broad peak assigned to the *N*-methyl group was observed at 3.25 ppm. The chemical shift of the peak maximum of the broad peak is reasonable as an average signal caused by exchange among one **Im** molecule coordinated from the inside of the C-3mer, two **Im** molecules coordinated from the outside of the C-3mer, and ca. 17 free **Im** molecules. The chemical shift of **Im** molecules coordinated with the outside and inside of the C-3mer was estimated to be 2.21 and –1.3 ppm, respectively, from the complex of monomeric C-3mer **1b** and 0.25 equiv of **Im** in $(CDCl_2)_2$, and from variable temperature NMR experiments of C-3mer with 0.5 equiv of **Im** at –40 °C. At room temperature, these coordinating **Im** molecules exchange rapidly with free **Im** molecules, whose *N*-methyl group was observed at 3.64 ppm, to give a broad signal at 3.25 ppm as an averaged signal. The addition of pyrene to the mixture caused a downfield shift of the signal, which almost stopped at

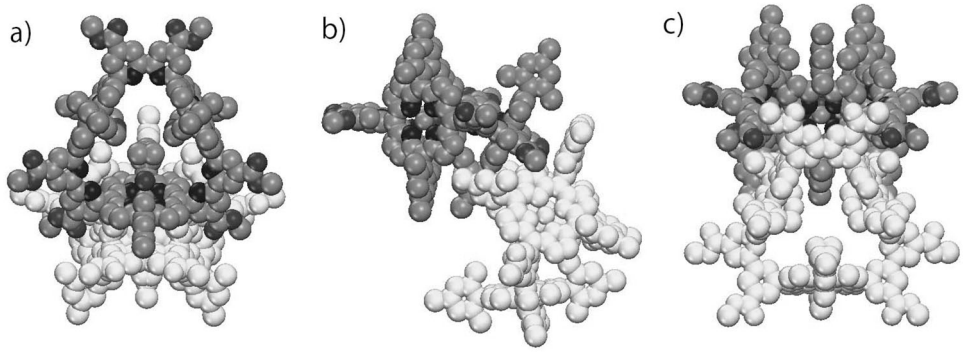

Figure 9. Molecular packing of 1a in the X-ray single crystal analysis; Hydrogen atoms are omitted for clarifying. A light color molecule is an adjacent one (1a). (a) a top view, (b) a side view, (c) a front view. The methyl group observed in the center of C-3mer in (a) is disordered at the two carbon positions.

3.32 ppm when ca. 20 equiv of pyrene had been added to the mixture (Figure S31). The resulting chemical shift is reasonable if three molecules are coordinated on the outside and no **Im** molecules **Im** exist on the inside.

The change in chemical shift of the pyrene molecules added during the titration also caused a downfield shift from the signals of the initial value on addition of 0.9 equiv of pyrene, and the signal eventually approached the value of free pyrene (Figure S32). These observations indicate that the pyrene molecules pushed out the **Im** molecules existing inside the C-3mer, and the pyrene molecules then became included inside the C-3mer as a host–guest complex. Based on molecular modeling, only one pyrene molecule can exist in the center of a cavity of C-3mer, and therefore, the observed change in chemical shift suggests that pyrene molecules in the system were exchanged.

Similarly, an NMR titration experiment of C-3mer **1b** with nitrobenzene was also carried out. Although the phenomenon of pushing out **Im** molecules from inside C-3mer was observed (Figure S33), no inclusion of nitrobenzene in the C-3mer was observed (Figure S34). This result also suggests that the mechanism of specific chromatographic separation of C-3mer on group C columns is different from that on group B columns. The inclusion of nonpolar π aromatic residues on the columns into the C-3mer, and dipole–dipole interactions of polar residues on the columns with the partial dipole moiety of the C-3mer are the most probable mechanisms for group B and C columns, respectively. Used as an eluent, pyridine has a dual role as a coordination ligand and as a polar solvent for each mechanism.

*Complexation of the bipyridyl parts in the C-3mer **1a***

Complexation of the bipyridyl parts in cyclic trimer **1a** was examined for various metal ions, using compounds such as Ni(II)Cl_2 and Cu(I)I, employing fluorescence spectroscopy. The addition of transition metal ions caused fluorescence quenching from cyclic trimer **1a**, suggesting a heavy metals effect after complexation of the metal ions with the bipyridyl parts of **1a**. For a more quantitative analysis, titration of **1a** with an η^3-allylpalladium tetrafluoroborate complex was carried out. To a solution of **1a** in $CHCl_3$ (0.38 mM), an η^3-allylpalladium tetrafluoroborate complex solution in $CHCl_3$ was added portionwise (0.5 equiv. each) of 6 equivalents to cyclic trimer **1a**. After stirring for 15 min after each addition, each aliquot was diluted 1,000 times to give a ca. 0.38 μM chloroform solution. UV-vis and fluorescence spectra of the diluted samples were collected (Figure 10). In the UV-vis spectra, the peak maximum of the Soret band had shifted toward the blue, from 425.5 to 422.5 nm, whereas the peak maxima of the Q-bands had shifted toward the red, from 560 and 606 to 564 and 630 nm, with significant broadening. At the same time, a successive absorption or scattering in the wavelength range from 320 to 700 nm was observed. In the fluorescence spectra, addition of 2 equiv. of a palladium complex resulted in an almost complete quenching of the fluorescence from **1a**. The mixture of **1a** with an η^3-allylpalladium tetrafluoroborate complex (6 equiv.) was analyzed using electron spray ionization (ESI) time-of-flight (TOF) mass spectrometry—ESI-TOF mass spectrometry and ^{1}H NMR spectroscopy in $CDCl_3$. From the ESI mass spectrum, [**1a**+ (allylpalladium)$_3$]$_3^+$ species and its derivatives were observed as dominant ones. (Figure S35) In the NMR spectrum (Figure 11b) comparing with **1a** and the η^3-allylpalladium tetrafluoroborate complex alone (Figures 11a and 11c) as references, characteristic η^3-allylpalladium species were observed at 1.8, –0.7, and –1.4 ppm, considered to be located within the cyclic porphyrin. Assignment of the allylpalladium species was performed using the coupling constants in the ^{1}H NMR, ^{1}H-^{1}H-COrrelation SpectroscopY (HH-COSY), NOESY, and HMQC spectra, as shown in Figure S36. Both NMR and ESI-mass data clearly shows formation of [**1a**-(allylPd)$_3$] complex as shown in Scheme 2. These complexation experiments indicate that the three bipyridyl parts can work as bidentate bisnitrogen ligands.

*Demetalation of zinc ions from C-3mer **1a** and incorporation of iron(III) ions*

To demonstrate that the three tetradentate porphyrinato parts in cyclic trimer **1a** also work as versatile ligands for multicofacial multimetalloporphyrin complexes, demetalation of the zinc ions from **1a** and incorporation of iron(III) ions was carried out. Iron porphyrins are well known as oxidation catalysts and as a model for cytochrome P450.[19] Treatment with trifluoroacetic acid (TFA)

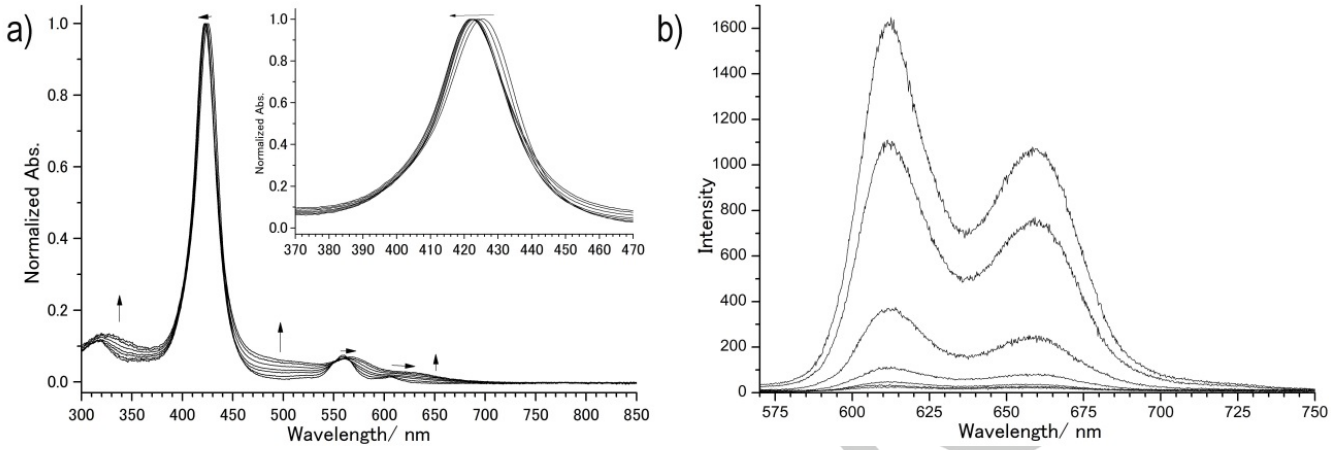

Figure 10. (a) UV-vis spectral change of **1a** by addition of an η^3-allylpalladium tetrafluoroborate complex in $CHCl_3$. (Normalized at the peak maxima of their Soret bands around 425 nm. Inset: the expanded spectra from 370 to 470 nm, (b) Fluorescence spectral changes of the same titration of (a) excited at 556 nm. (Their intensities are normalized by dividing with the absorbance at the excited wavelength.

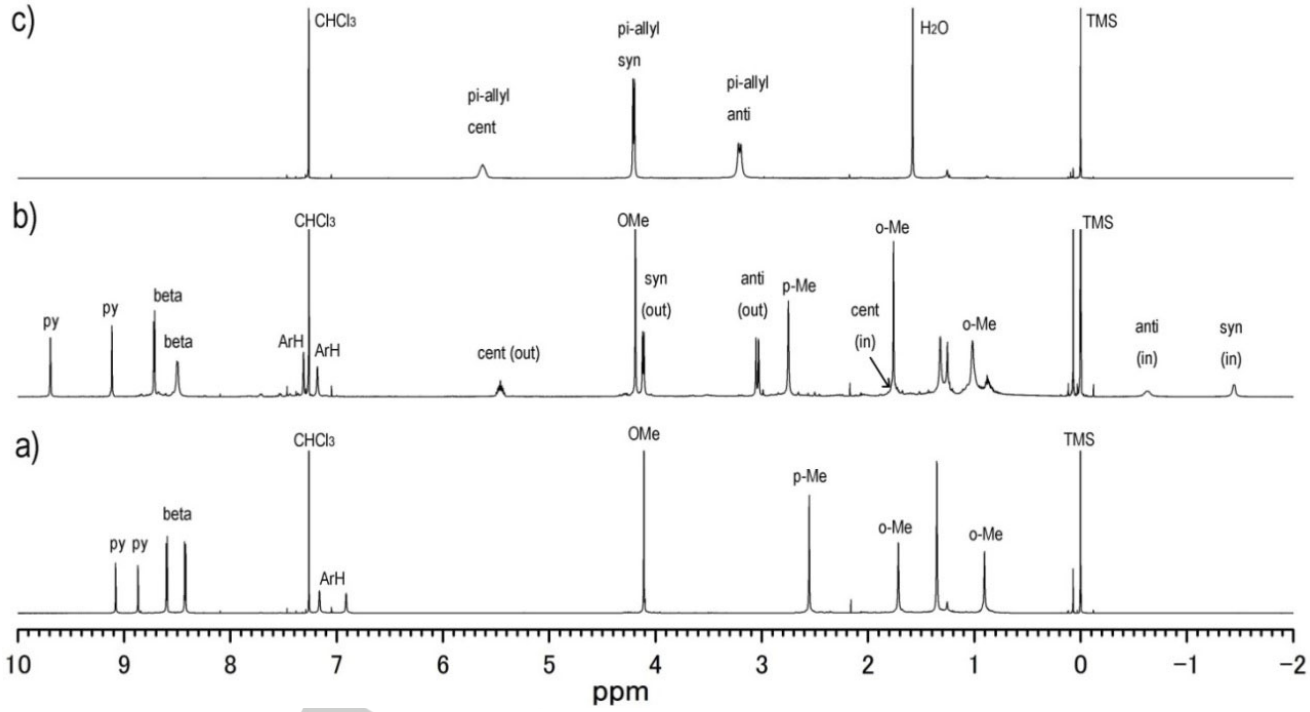

Figure 11. ^{1}H NMR spectra (500 MHz, in $CDCl_3$) of (a) **1a**, (b) a mixture of **1a** with η^3-allylpalladium tetrafluoroborate complex (6 equiv.), and (c) η^3-allylpalladium tetrafluoroborate complex.

and conc. H_2SO_4 of **1a** in dry $CHCl_3$ at 0 °C, followed by neutralization with $NaHCO_3$ gave the freebase porphyrin **6a**. The structure of **6a** was confirmed using NMR (Figures S37 and S38) and high-resolution MALDI-TOF mass analysis (Figures S39 and S40). Its D_{3h} symmetric structure was observed in the NMR spectrum. Treatment of $Fe(CO)_5$ and iodine with **6a** in toluene, followed by ligand exchange with a 1 M HCl solution gave corresponding iron(III) C-3mer **7a**. (Scheme 3) The structural analysis was performed by UV-vis spectrum and MALDI-TOF mass spectrum as shown in Figures S41 and S42. This observation suggests that the C-3mers **1** are precursors for cyclic tris metallo porphyrin derivatives.

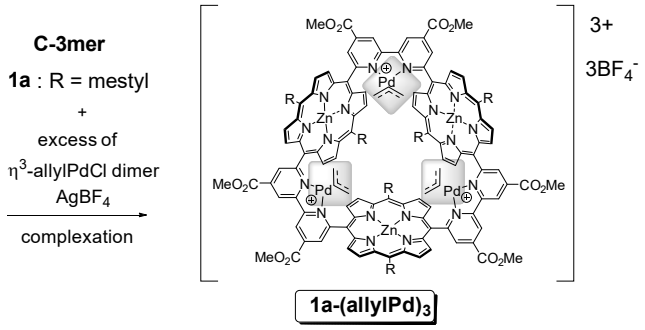

Scheme 2. Complexation of an η^3-allylpalladium complex with C-3mer **1a**

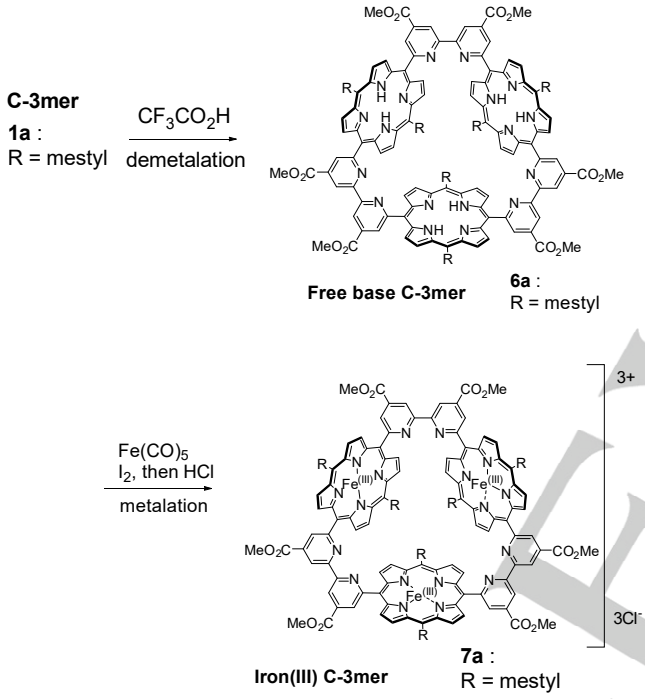

Scheme 3. Demetalation of **1a** (R=mesityl) into free base C-3mer **6a** and incorporation of iron(III) ion into 6a to give iron(III) C-3mer **7a**.

Conclusions

One-step synthesis of D_{3h} symmetric cyclic porphyrin trimers **1** was achieved from a nickel-mediated reductive coupling of bis(chloropyridyl)porphyrinatozinc **2**. Although the cyclic trimers **1** were obtained as a mixture that contained other cyclic and acyclic porphyrin oligomers, the cyclic trimers **1** could be isolated efficiently from the mixtures using cyanopropyl-modified silica gel column chromatography. Structural analysis of the cyclic trimers **1** was carried out using NMR spectroscopy and X-ray crystallography. As a result, in solution, the cyclic trimers were found to assume an apparent D_{3h} symmetric macrocyclic structure in which three bipyridyl parts are directed toward the center, and six carboxylic ester groups exist outside the ring. Treatment of an η^3-allylpalladium complex with cyclic trimer **1a** gave a trispalladium complex **1a**-(allylPd)$_3$, indicating the bipyridyl moieties inside the ring could work as bidentate metalloligands. The zinc porphyrin parts also worked as tetradentate metallo ligands of an iron porphyrin complex after acidic demetalation of the zinc ions. These demonstrations show that the cyclic trimers **1** are versatile macrocyclic ligands for multicofacial multimetallic complexes. Unique catalytic activity using multimetallic sites within their restricted ca. one-nanometer space is expected.

From the effect of the solvents chloroform and pyridine on PYE columns and the NMR titration experiments of C-3mer **1b** with pyrene, the following interesting relationship between chloroform, pyridine, and pyrene in C-3mer was revealed. Although pyrene molecules alone cannot push out chloroform molecules held in C-3mer, this becomes possible with the assistance of a coordinating solvent, such as pyridine. The coordination of pyridine with the zinc ions in the C-3mer overcomes the interaction of chloroform molecules inside the C-3mer, and the exchange rate of the coordination bond between the inside and outside moieties is rapid. Then, pyrene molecules can be inserted inside the C-3mer. Such a cooperative effect to form a host–guest complex is unique. The two different separation mechanisms for C-3mer observed on group B and C columns will be applicable for isolation of other macrocyclic compounds, and a combination of the methods will allow new strategies to be pursued to prepare various macrocycles.

Experimental Section

Synthesis of 1a. In a 200 mL of Schlenk flask overflowing with Ar, Ni(cod)$_2$ (174 mg, 0.63 mmol) and 2,2'-bipyridyl (101 mg, 0.65 mmol) were placed. Dry DMF (60 mL) was added to the mixture, and the mixture was stirred for 5 min at 25 ˚C to give dark purple solution. Porphyrinatozinc **2a** (30.7 mg, 0.032 mmol) and dry DMF (29 mL) were added to the mixture and stirred under argon for 16 h at 50 ˚C. To the mixture, $CHCl_3$ (20 mL) was added, and the mixture was washed with an aqueous citric acid solution (0.3 M, 80 mL) by four times. Subsequently, the organic layer was washed with an aqueous NH_4OH solution (25%, 20 mL) by three times. The organic layer was filtered through a membrane filter (Omnipore, 0.1 μm), and the filtrate was concentrated to give purple solid (33.3 mg). The crude mixture was purified on Cyanogel (Yamazen YFLC Gel, 40 μm dp, 60 Å pore) column chromatography using a mixture of toluene and pyridine (15/85 vol/vol) as an eluent to give **1a** (5.5 mg). This sample was recrystallized from 2-butanone and methanol to afford pure **1a** (3.7 mg, 13.1%). All of the ^{1}H and ^{13}C NMR signals in $CDCl_3$ were assigned as shown in Figure 7. The 1D and 2D NMR data are shown in Figures 6, and S11-S14. MALDI-TOF-MS (dithranol) *m/z* 2651.7112 $(M+Na)^+$, calcd for $[C_{156}H_{120}N_{18}O_{12}Zn_3+Na]^+$ 2651.7100. The datum is shown in Figure S15. UV-vis (max/nm (ε / M^{-1} cm^{-1}), pyridine) 432.2 (7.0 x 10^5), 564.2 (4.3 x 10^4), 610.2 (1.3 x 10^4).

Allylpalladium complex 1a-(allylPd)$_3$. A stock solution of η^3-allylpalladium tetrafluoroborate complex was prepared from η^3-allylpalladium chloride dimer (3.9 mg, 11 μmol) and silver tetrafluoroborate (7.3 mg, 37 μmol) in chloroform (1.0 mL) at 0 ºC. To a solution of **1a** (1.0 mg, 0.38 μmol) in degassed $CHCl_3$ (1.0 mL), the above stock solution was added portionwise with 0.5 equiv. each by 6 equivalents to cyclic trimer **1a**. After 15 min stirring for each addition, each aliquot was diluted by 1,000 times to give ca. 0.38 μM chloroform

solution. UV-vis and fluorescence spectra of the diluted sample were collected. (see text and Figure 10). A mixture of **1a** and 6 equiv. of η^3-allylpalladium tetrafluoroborate complex was analyzed by ESI-mass spectrometry and ^{1}H NMR spectroscopy. (see text and Figures S35 and 11b)

Demetalation of zincporphyrin 1a to freebase porphyrin 6a. To a solution of **1a** (5.0 mg) in dry chloroform (2.0 mL), trifluoroacetic acid (TFA, 2.0 mL) was added dropwise at 0 ºC to give green solution. Subsequently, conc. H_2SO_4 (0.2 mL) was added dropwise to give pale brown suspension. The reaction mixture was added to a saturated $NaHCO_3$ solution to maintain pH 8~9. The organic layer was extracted with chloroform, dried over anhydrous Na_2SO_4, and concentrated under reduced pressure. The residue was purified by short flash SiO_2 column chromatography to give free base C-3mer **6a** (4.0 mg) as a brown solid. ^{1}H NMR (300 MHz, $CDCl_3$) δ (ppm) 9.09 (d, 2H, *J* = 1.4 Hz), 8.87 (d, 2H, *J* = 1.4 Hz), 8.57 (d, 4H, *J* = 4.6 Hz), 8.36 (d, 4H, *J* = 4.6 Hz), 7.07 (br, 2H), 6.85 (br, 2H), 4.13 (s, 6H), 2.55 (s, 6H), 1.73 (s, 6H), 1.01 (s, 6H), -3.17 (s, 2H). ^{13}C NMR (75 MHz, $CDCl_3$) δ (ppm) 166.14 (C=O), 162.91 (C), 156.48 (C), 139 (broad), 138.26 (C), 137.41 (C), 136.94 (C), 131 (broad), 128.49 (CH), 127.58 (CH), 121.06 (CH), 118.27 (C), 116.88 (C), 53.22 (CH_3), 21.51 (CH_3). MALDI-TOF-MS (dithranol) *m/z* 2443.9812 $(M+H)^+$, calcd for $[C_{156}H_{126}N_{18}O_{12}+H]^+$ 2443.9875, 2465.9697 $(M+Na)^+$, calcd for $[C_{156}H_{126}N_{18}O_{12}+Na]^+$ 2465.9695. UV-vis (max/nm, $CHCl_3$) 419.9, 516.5, 591.4, 647.5.

Synthesis of iron(III)porphyrin 7a. To a solution of **6a** (6.5 mg, 2.7 μmol) in toluene (10.0 mL), excess amounts of I_2 (76.5 mg) was added under Ar. To the mixture, excess amounts of $Fe(CO)_5$ solution (40 μL) was added. After 5 min. stirring at rt, the mixture was heated at 60 ºC for 1 h under Ar atmosphere. At 0 ºC, 1 M HCl solution was added to the mixture, and the mixture was stirred for 5 min. The organic layer was washed with distilled water and brine, dried over anhydrous Na_2SO_4, and concentrated under reduced pressure to give **7a** (6.7 mg). This sample was analyzed by MALDI-TOF mass spectrometry and UV-vis spectrometer as shown in Figures S42 and S43, and Figure S41, respectively. UV-vis (max/nm (Abs.), $CHCl_3$) 380.0 (0.270), 420.2 (0.435), 515.0 (0.077), 580.0 (0.026), 670.0 (0.014).

Acknowledgements

A.S. thanks financial support by KAKENHI (24510140) from the Japan Society for the Promotion of Science (JSPS).

Keywords: porphyrin • macrocycle • bipyridine • multinuclear complex • chromatography

[1] a) L. G. Mackay, R. S. Wylie and J. K. M. Sanders, J. Am. Chem. Soc. 1994, 116, 3141-3142; b) M. Marty, Z. Clyde-Watson, L. J. Twyman, M. Nakash and J. K. M. Sanders, *Chem. Commun.* **1998**, 2265-2266; c) M. Yoshizawa, T. Kusukawa, M. Fujita and K. Yamaguchi, *J. Am. Chem. Soc.* **2000**, *122*, 6311-6312; d) M. L. Merlau, M. del Pilar Mejia, S. T. Nguyen and J. T. Hupp, *Angew. Chem.* **2001**, *113*, 4369-43; *Angew. Chem. Int. Ed.* **2001**, *40*, 4239-4242; e) M. Yoshizawa, T. Kusukawa, M. Fujita, S. Sakamoto and K. Yamaguchi, *J. Am. Chem. Soc.* **2001**, *123*, 10454-10459; f) P. Thordarson, E. J. A. Bijsterveld, A. E. Rowan and R. J. M. Nolte, *Nature* **2003**, *424*, 915-918; g) D. Fiedler, D. H. Leung, R. G. Bergman and K. N. Raymond, *Acc. Chem. Res.* **2004**, *38*, 349-358; h) D. Fiedler, R. G. Bergman and K. N. Raymond, *Angew. Chem.* **2004**, *116*, 6916-19; *Angew. Chem. Int. Ed.* **2004**, *43*, 6748-6751; i) D. M. Vriezema, M. Comellas Aragonès, J. A. A. W. Elemans, J. J. L. M. Cornelissen, A. E. Rowan and R. J. M. Nolte, *Chem. Rev.* **2005**, *105*, 1445-1490; j) M. Kuil, T. Soltner, P. W. N. M. van Leeuwen and J. N. H. Reek, *J. Am. Chem. Soc.* **2006**, *128*, 11344-11345; k) S. Jonsson, F. G. J. Odille, P.-O. Norrby and K. Warnmark, *Org. Biomol. Chem.* **2006**, *4*, 1927-1948; l) M. D. Pluth, R. G. Bergman and K. N. Raymond, *Science* **2007**, *316*, 85-88; m) S. J. Lee, K. L. Mulfort, X. Zuo, A. J. Goshe, P. J. Wesson, S. T. Nguyen, J. T. Hupp and D. M. Tiede, *J. Am. Chem. Soc.* **2007**, *130*, 836-838; n) S. J. Lee, S.-H. Cho, K. L. Mulfort, D. M. Tiede, J. T. Hupp and S. T. Nguyen, *J. Am. Chem. Soc.* **2008**, *130*, 16828-16829; o) M. Yoshizawa, J. K. Klosterman and M. Fujita, *Angew. Chem.* **2009**, *121*, 3470-90; *Angew. Chem. Int. Ed.* **2009**, *48*, 3418-3438; p) K. Oisaki, Q. Li, H. Furukawa, A. U. Czaja and O. M. Yaghi, *J. Am. Chem. Soc.* **2010**, *132*, 9262-9264; q) T. Murase and M. Fujita, *The Chemical Record* **2010**, *10*, 342-347; r) T. R. Cook, Y.-R. Zheng and P. J. Stang, *Chem. Rev.* **2012**, *113*, 734-777; s) H. Amouri, C. Desmarets and J. Moussa, *Chem. Rev.* **2012**, *112*, 2015-2041; t) M. Guitet, P. Zhang, F. Marcelo, C. Tugny, J. Jiménez-Barbero, O. Buriez, C. Amatore, V. Mouriès-Mansuy, J.-P. Goddard, L. Fensterbank, Y. Zhang, S. Roland, M. Ménand and M. Sollogoub, *Angew. Chem.* **2013**, *125*, 7354-59; *Angew. Chem. Int. Ed.* **2013**, *52*, 7213-7218; u) J. Hong, K. E. Djernes, I. Lee, R. J. Hooley and F. Zaera, *ACS Catal.* **2013**, *3*, 2154-2157; v) J. Liu, L. Chen, H. Cui, J. Zhang, L. Zhang and C.-Y. Su, *Chem. Soc. Rev.* **2014**, *43*, 6011-6061; w) C. Zhao, F. D. Toste, K. N. Raymond and R. G. Bergman, *J. Am. Chem. Soc.* **2014**, *136*, 14409-14412.

[2] a) R. D. Adams, F. A. Cotton, *Catalysis by Di- and Polynuclear Metal Cluster Complexes*; Wiley, **1998**; b) N. C. Gianneschi, P. A. Bertin, S. T. Nguyen, C. A. Mirkin, L. N. Zakharov and A. L. Rheingold, *J. Am. Chem. Soc.* **2003**, 125, 10508-10509; c) N. Tsukada, S. Ninomiya, Y. Aoyama and Y. Inoue, *Pure Appl. Chem.* **2008**, *80*, 1161-1166; d) X. Liu and W. Chen, *Organometallics* **2012**, *31*, 6614-6622; e) S. Takano, D. Takeuchi, K. Osakada, N. Akamatsu and A. Shishido, *Angew. Chem.* **2014**, *126*, 9400-04; *Angew. Chem. Int. Ed.* **2014**, *53*, 9246-9250.

[3] a) S. J. Lee, A. Hu and W. Lin, *J. Am. Chem. Soc.* **2002**, *124*, 12948-12949; b) A. M. Appel, J. E. Bercaw, A. B. Bocarsly, H. Dobbek, D. L. DuBois, M. Dupuis, J. G. Ferry, E. Fujita, R. Hille, P. J. A. Kenis, C. A. Kerfeld, R. H. Morris, C. H. F. Peden, A. R. Portis, S. W. Ragsdale, T. B. Rauchfuss, J. N. H. Reek, L. C. Seefeldt, R. K. Thauer and G. L. Waldrop, *Chem. Rev.* **2013**, *113*, 6621-6658; c) P. Buchwalter, J. Rosé and P. Braunstein, *Chem. Rev.* **2014**, *115*, 28-126.

[4] a) A. Kless, C. Lefeber, A. Spannenberg, R. Kempe, W. Baumann, J. Holz and A. Börner, *Tetrahedron* **1996**, *52*, 14599-14606; b) Q. F. Mokuolu, P. A. Duckmanton, P. B. Hitchcock, C. Wilson, A. J. Blake, L. Shukla and J. B. Love, *Dalton Trans.* **2004**, 1960-1970.

[5] a) X. Sun, D. W. Johnson, D. L. Caulder, R. E. Powers, K. N. Raymond and E. H. Wong, *Angew. Chem.* **1999**, *111*, 1689-94; *Angew. Chem. Int. Ed.* **1999**, *38*, 1303-1307; b) S. Abe, J. Niemeyer, M. Abe, Y. Takezawa, T. Ueno, T. Hikage, G. Erker and Y. Watanabe, *J. Am. Chem. Soc.* **2008**, *130*, 10512-10514; c) J. Moussa and H. Amouri, *Angew. Chem.* **2008**, *120*, 1392-1400; *Angew. Chem. Int. Ed.* **2008**, *47*, 1372-1380; d) R. Maity, A. Rit, C. Schulte to Brinke, C. G. Daniliuc and F. E. Hahn, *Chem. Commun.* **2013**, *49*, 1011-1013.

[6] a) Z. Clyde-Watson, A. Vidal-Ferran, L. J. Twyman, C. J. Walter, D. W. J. McCallien, S. Fanni, N. Bampos, R. Stephen Wylie and J. K. M. Sanders, *New J. Chem.* **1998**, *22*, 493-502; b) R. Gramage-Doria, D. Armspach and D. Matt, Coord. *Chem. Rev.* **2013**, *257*, 776-816; c) T. Nabeshima and M. Yamamura, *Pure Appl. Chem.* **2013**, *85*, 763-776; d) K. Omoto, S. Tashiro, M. Kuritani and M. Shionoya, *J. Am. Chem. Soc.* **2014**, *136*, 17946-17949.

[7] a) J. E. Hutchison, T. A. Postlethwaite, C.-h. Chen, K. W. Hathcock, R. S. Ingram, W. Ou, R. W. Linton, R. W. Murray, D. A. Tyvoll, L. L. Chng and J. P. Collman, *Langmuir* **1997**, *13*, 2143-2148; b) C. J. Chang, Y. Deng, A. F. Heyduk, C. K. Chang and D. G. Nocera, *Inorg. Chem.* **2000**, *39*, 959-966; c) S. Faure, C. Stern, R. Guilard and P. D. Harvey, *J. Am. Chem. Soc.* **2004**, *126*, 1253-1261; d) P. Peljo, L. Murtomäki, T. Kallio,

H.-J. Xu, M. Meyer, C. P. Gros, J.-M. Barbe, H. H. Girault, K. Laasonen and K. Kontturi, *J. Am. Chem. Soc.* **2012**, *134*, 5974-5984.

[8] S. Durot, J. Taesch and V. Heitz, *Chem. Rev.* **2014**, *114*, 8542-8578.

[9] a) C. N. Hunter, F. Daldal, M. C. Thurnauer, J. T. Beatty in *The Purple Phototrophic Bacteria, Series: Advances in Photosynthesis and Respiration*; Springer: Dordrecht, **2009**; Vol. 28; b) N. Aratani, D. Kim and A. Osuka, *Acc. Chem. Res.* **2009**, *42*, 1922-1934; c) A. Satake in *Handbook of Porphyrins: Chemistry, Properties and Applications*; (Eds.; A. Kaibara, G. Matsumara) Nova Science Publishers: **2012**, p 409-428; d) P. Parkinson, C. E. I. Knappke, N. Kamonsutthipaijit, K. Sirithip, J. D. Matichak, H. L. Anderson and L. M. Herz, *J. Am. Chem. Soc.* **2014**, *136*, 8217-8220.

[10] a) H. L. Anderson and J. K. M. Sanders, *J. Chem. Soc., Chem. Commun.***1989**, 1714-1715; b) J. K. M. Sanders in *Comprehensive Supramolecular Chemistry*, Vol. 9 (Eds. J.-P. Sauvage, M. W. Hosseini) Elsevier, Oxford, UK., **1996**, pp. 131–164; c) A. L. Kieran, A. D. Bond, A. M. Belenguer and J. K. M. Sanders, *Chem. Commun.* **2003**, 2674-2675; d) J. X. Song, N. Aratani, H. Shinokubo and A. Osuka, *J. Am. Chem. Soc.* **2010**, *132*, 16356-16357; e) G. n. Gil-Ramírez, S. D. Karlen, A. Shundo, K. Porfyrakis, Y. Ito, G. A. D. Briggs, J. J. L. Morton and H. L. Anderson, *Org. Lett.* **2010**, *12*, 3544-3547.

[11] A. Satake, M. Yamamura, M. Oda and Y. Kobuke, *J. Am. Chem. Soc.* **2008**, *130*, 6314-6315.

[12] a) O. Mongin, A. Schuwey, M. A. Vallot and A. Gossauer, *Tetrahedron Lett.* **1999**, *40*, 8347-8350; b) T. Hori, N. Aratani, A. Takagi, T. Matsumoto, T. Kawai, M. C. Yoon, Z. S. Yoon, S. Cho, D. Kim and A. Osuka, *Chem. Eur. J.* **2006**, *12*, 1319-1327; c) M. Hoffmann, C. J. Wilson, B. Odell and H. L. Anderson, *Angew. Chem.* **2007**, *119*, 3183-86; *Angew. Chem. Int. Ed.* **2007**, *46*, 3122-3125.

[13] a) J. Z. Li, A. Ambroise, S. I. Yang, J. R. Diers, J. Seth, C. R. Wack, D. F. Bocian, D. Holten and J. S. Lindsey, *J. Am. Chem. Soc.* **1999**, *121*, 8927-8940; b) C. Ikeda, A. Satake and Y. Kobuke, *Org. Lett.* **2003**, *5*, 4935-4938; c) A. Kato, K. Sugiura, H. Miyasaka, H. Tanaka, T. Kawai, M. Sugimoto and M. Yamashita, *Chem. Lett.* **2004**, *33*, 578-579; d) S. Rucareanu, A. Schuwey and A. Gossauer, *J. Am. Chem. Soc.* **2006**, *128*, 3396-3413; e) S.-i. Sasaki and H. Tamiaki, *Tetrahedron Lett.* **2006**, *47*, 4965-4968; f) M. Hoffmann, J. Kärnbratt, M.-H. Chang, L. M. Herz, B. Albinsson and H. L. Anderson, *Angew. Chem.* **2008**, *120*, 5071-74; *Angew. Chem. Int. Ed.* **2008**, *47*, 4993-4996; g) E. Scamporrino, P. Mineo and D. Vitalini, *Tetrahedron* **2011**, *67*, 3705-3713.

[14] a) O. Shoji, S. Okada, A. Satake and Y. Kobuke, *J. Am. Chem. Soc.* **2005**, *127*, 2201-2210; b) H. Jiang and W. Lin, *J. Am. Chem. Soc.* **2006**, *128*, 11286-11297; c) Y. Kuramochi, A. Satake, M. Itou, K. Ogawa, Y. Araki, O. Ito and Y. Kobuke, *Chem. Eur. J.* **2008**, *14*, 2827-2841; d) T. Hori, X. Peng, N. Aratani, A. Takagi, T. Matsumoto, T. Kawai, Z. S. Yoon, M.-C. Yoon, J. Yang, D. Kim and A. Osuka, *Chem. Eur. J.* **2008**, *14*, 582-595.

[15] a) Y. Tomohiro, A. Satake and Y. Kobuke, *J. Org. Chem.* **2001**, *66*, 8442-8446; b) H. Kitagishi, A. Satake and Y. Kobuke, *Inorg. Chem.* **2004**, *43*, 3394-3405; c) S. Fukuda, A. Satake and Y. Kobuke, *Thin Solid Films* **2006**, *499*, 263-268.

[16] T. Yamamoto, S. Wakabayashi and K. Osakada, *J. Organomet. Chem.* **1992**, *428*, 223-237.

[17] L. R. Snyder, *J. Chromatogr. A* **1974**, *92*, 223-230.

[18] H. Imai, S. Nakagawa and E. Kyuno, *J. Am. Chem. Soc.* **1992**, *114*, 6719-6723.

[19] a) K. S. Suslick, In *The Porphyrin Handbook* (Eds.; K. M. Kadish, K. M. Smith, R. Guilard) Academic Press: New York, **2000**; Vol. 4, pp 41-63; b) J. T. Groves, K. Shalyaev, J. Lee, In *The Porphyrin Handbook* (Eds.; K. M. Kadish, K. M. Smith, R. Guilard) Academic Press: New York, **2000**; Vol. 4, pp 17-40; c) F. A. Walker, U. Simonis, In *Encyclopedia of Inorganic and Bioinorganic Chemistry*; John Wiley & Sons, Ltd: **2011**.

FULL PAPER

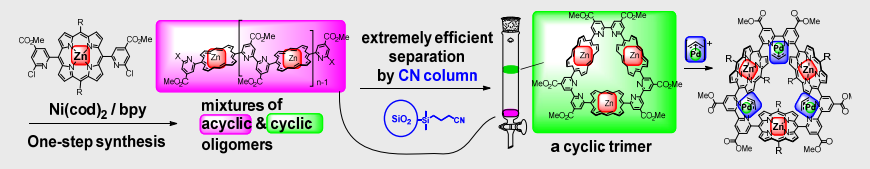

Chromatography on a cyanopropyl-modified column supplied a cyclic porphyrin trimer efficiently from a mixture of acyclic and cyclic oligomers. Treatment of an η^3-allylpalladium complex with the cyclic trimer gave a trispalladium complex, indicating that the cyclic trimer is versatile macrocyclic ligands for multicofacial multimetallic complexes.

Yohei Ohkoda, Akane Asaishi, Tomoya Namiki, Tomoaki Hashimoto, Midori Yamada, Koichiro Shirai, Yuta Katagami, Tomoaki Sugaya, Makoto Tadokoro, and Akiharu Satake**

Page No. – Page No.

D_{3h} Symmetric Porphyrin-Based Rigid Macrocyclic Ligands for Multicofacial Multinuclear Complexes in a One-Nanometer-Size Cavity